Time-delay feedback control of a suspended cable driven by subharmonic and superharmonic resonance

Time-delay feedback control of a suspended cable driven by subharmonic and superharmonic resonance

Jian Peng[a,b,*], Yanan Li[a], Luxin Li[a,c], Stefano Lenci[d] and Hongxin Sun[a,*]

[a]School of Civil Engineering, Hunan University of Science and Technology, Xiangtan, Hunan 411201, PR China
[b]Hunan Provincial Key Laboratory of Structures for Wind Resistance and Vibration Control, Hunan University of Science and Technology, Xiangtan, Hunan 411201, PR China
[c]School of Civil Engineering and Communication, North China University of Water Resources and Electric Power, Zhengzhou 450045, China
[d]Department of Civil and Building Engineering and Architecture, Polytechnic University of Marche, Ancona 60131, Italy

ARTICLE INFO

Keywords:
suspended cable
time-delay feedback
subharmonic
superharmonic resonance
vibration control

ABSTRACT

The longitudinal time-delay feedback control strategy is implemented to suppress the subharmonic and superharmonic responses of the suspended cable. Formulated based on the Hamilton variational principle and the longitudinal time-delay feedback strategy, the in-plane nonlinear differential equations for a suspended cable are formulated, and Galerkin method is utilized to transform the equations into delayed differential equations. By using the method of multiple scales, approximate solutions for the 1/2-subharmonic and second-order superharmonic resonance responses of the controlled suspended cable were derived. The effects of the time delay and control gain are obtained through numerical examples. The research results demonstrate that through the adjustment of control gain and time delay, resonance regions can be avoided, effectively suppressing large-amplitude vibrations in the suspended cable, thereby achieving favorable control performance.

1. Introduction

The suspended cable, renowned for their rational force distribution, material efficiency, swift construction, and aesthetic design, find widespread application in large-span structures including suspension bridges, sports arena roofs, and transmission lines[1]. However, the low damping, light mass, and high flexibility of suspended cables make them prone to experiencing significant vibrations under external loads, resulting in structural fatigue and damage[2; 3].

Therefore, on one hand, the vibration control issue of suspended cable has been a focal point of attention. The current methods for vibration control of suspended cable mainly include the implementation of aerodynamic measures[4; 5], auxiliary cable measures[6; 7], and utilizing dampers for vibration control. The damper control method is the most common approach for vibration control in structural engineering. They can be categorized into passive control methods (such as MR dampers[8]),active control methods (such as AMD dampers[9] and PPF control strategy[10]), semi-active control methods (such as AVS systems[11]), and intelligent control methods (such as piezoelectric material MEMS[12; 13]). Active control, utilizing transverse and longitudinal boundary motion for vibration control, has garnered widespread attention and application due to its high precision and wide control range. In [14; 15], extensive research was conducted on the nonlinear vibration issues of controlled suspended cables under in-plane excitation based on the single support longitudinal displacement active control method. Subsequently, further exploration was carried out by applying longitudinal forces at the supports to analyze, predict, and experimentally validate the cable's vibration response under longitudinal control. Following this, in [16], an active controller for out-of-plane vibration of flexible cables was developed based on boundary actuators and sensors, achieving gradual stability of cable displacement while compensating for uncertainties in actuator mass and cable tension parameters. With the development of cable structure spans, modeling and control research on flexible transport systems with arbitrary variations in cable length under longitudinal vibration control were conducted in [17]. Addressing actual load conditions, active control of cable vibrations under lateral wind effects was achieved by applying longitudinal motion to supports, as described in [18]. Recently, seismic probabilistic assessments under longitudinal control have been conducted on system-based tall tower cable-stayed bridge models, as reported in [19]. The vibration control

*Corresponding author.
Pengjian@hnu.edu.cn (J. Peng); cehxsun@hnust.edu.cn (H. Sun)
ORCID(s):

research for dampers predominantly focuses on the linear aspects. Moreover, in existing active control strategies, it should be noted that the controller itself, signal processing, and actuators all possess certain time delays, and the existence of time delays may result in the input of energy to the system when it is not required, there by leading to a reduction in the performance of control dampers[20; 21]. To mitigate the influence of time delay and enhance the performance of the control system, a novel active control method time-delay vibration reduction method has been proposed[22]. Recently this method has been further developed to effectively exploit but unavoidable time delays in the feedback loop, creating the so-called multi-delay distributed time-delay absorber (MD-DDR) to achieve complete vibration suppression[23]. Therefore, the time-delay feedback control, as an effective control method, has been widely applied in the field of structural vibration control[24; 25].

On the other hand, notable nonlinear phenomena are present in engineering structures[26; 27]. For suspended cable, the existence of quadratic and cubic nonlinear terms renders their nonlinear characteristics significantly pronounced. When subjected to deterministic or random external loads, the suspended cable exhibits complex nonlinear dynamic behavior due to its inherent flexibility and nonlinear effects in other local regions of the structure[28–32]. Under external loads, the suspended cable is prone to undergo multi-mode vibrations, with energy exchanging between multiple modal orders. In practical engineering, occurrences of subharmonic resonance and superharmonic resonance have been observed[33–37].

In summary, the exploration of nonlinear vibration control in suspended cable systems is considered of paramount significance in engineering practice. Moreover, subharmonic and superharmonic resonance phenomena are prevalent in practical applications, underscoring the necessity for comprehensive investigation. Thus, an innovative approach, inspired by [38] and guided by the perspective presented in [39], is adopted in this study, focusing on considerations of longitudinal time-delayed vibration control. The primary objective is to analyze the nonlinear sub-resonance response of suspended cables under longitudinal time-delayed feedback control, with the aim of optimizing the design and implementation of such control strategies to enhance dynamic performance. In Section 2, the inquiry is initiated by deriving the nonlinear motion differential equations of the controlled suspended cable through the application of the Hamiltonian variational principle. Subsequently, Galerkin discretization is employed to transform these equations into delay differential equations, marking a novel methodological contribution. Sections 3 and 4 delve into the examination of 1/2-subharmonic resonance and second-order superharmonic resonance, respectively, utilizing the method of multiple scales. Through numerical examples, in-depth parameter analysis of the control system is conducted, scrutinizing variables such as control gains, time delays, and other influential factors. Finally, Section 5 consolidates the findings and presents a series of conclusions, encapsulating the innovative contributions and implications of this study.

2. Mathematical Model

As shown in Fig.1, the cable is suspended on two supports located on the same horizontal line in the *O-xy* coordinate plane. The coordinate origin O is located on one side of the suspended cable. It is assumed that the cross-sectional area of the suspended cable remains constant along the length direction, and the suspended cable always stays within the range of elastic deformation. By using the Hamilton variational principle, the in-plane nonlinear motion equation of the suspended cable can be obtained by neglecting its bending stiffness, torsional stiffness, and shear stiffness. The equation is given by

$$m\ddot{v} + 2c\dot{v} - Hv'' - \frac{EA}{L}(y'' + v'')\left[u_c + \int_0^L (y'v' + \frac{1}{2}v'^2)dx\right] = F(x,t), \tag{1}$$

where m is the mass per unit length of the suspended cable; c is the damping coefficient of the suspended cable; E is the elastic modulus of the suspended cable; A is the cross-sectional area of the suspended cable; L is the span of the suspended cable; H is the horizontal tension of the suspended cable ($H = mgL^2/8b, H \leq EA$), b is the sag; g is the acceleration due to gravity; u_c is the longitudinal displacement applied to the right end moving support; $F(x,t) = P(x)\cos(\Omega t)$ is the external excitation; Ω is the frequency of the external excitation; $P(x)$ is the distribution function of the external excitation.

It is assumed that the sag-to-span ratio of the suspended cable is relatively small ($b/L < 1/8$), so its shape can be described as a parabola

$$y(x) = 4b\left[x/L - (x/L)^2\right].$$

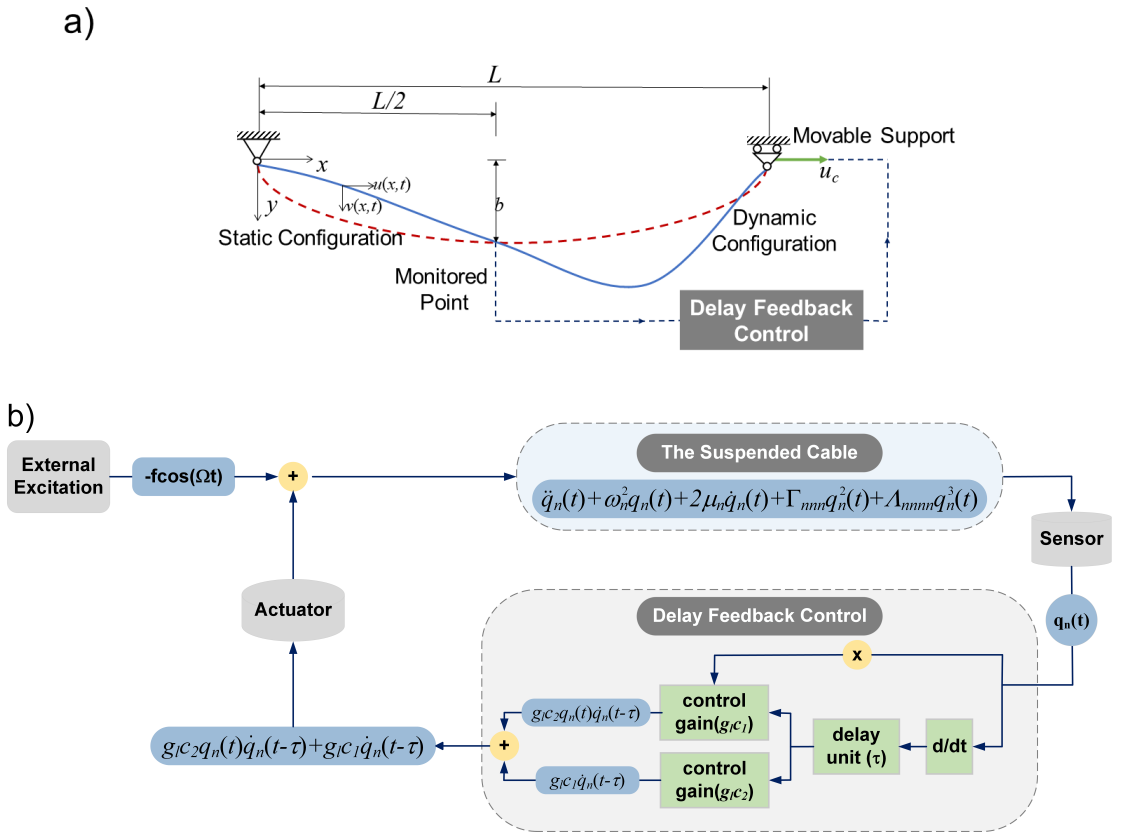

Figure 1: The schematic of the controlled suspended cable and operating system. a)Controlled suspended cable; b)Schematic diagram of the whole system.

In this paper, the linear velocity time-delay feedback strategy is used for vibration control, which can be expressed as

$$u_c(t) = g_l \dot{v}(x_c, t-\tau),$$

where g_l is the control gain and τ is the time-delay of the control system, respectively.

Introducing dimensionless parameters

$$x^* = x/L, y^* = y/L, v^* = v/L, \alpha = EA/H, P^* = PL/H,$$
$$t^* = t\sqrt{g}/8b, \Omega^* = \Omega\sqrt{8b/g}, c^* = (c/m)\sqrt{8b/g}, g_l{}^* = g_l/L, \tau^* = \tau\sqrt{g/8b}.$$

After nondimensionalization, the motion equation can be expressed as

$$\ddot{v} + 2c\dot{v} - v'' - \alpha(y'' + v'')\left[u_c + \int_0^L (y'v' + \frac{1}{2}v'^2)dx\right] = P(x)\cos(\Omega t), \tag{2}$$

for convenience of writing, the art in Eq.(2) have been removed.

The Galerkin method is used to discretize Eq.(2), assuming the nondimensional displacement function after nondimensionalization as

$$v(x,t) = \sum_{n=1}^{\infty} q_n(t)\phi_n(x), \tag{3}$$

where $q_n(t)$ is the vibration function of displacement, $\phi_n(x)$ is the mode function[39]. Substituting Eq.(3) into Eq.(2), we have

$$\begin{aligned}&\ddot{q}_n(t)+\omega_n^2 q_n(t)+2\mu_n\dot{q}_n(t)+\sum_{i,j=1}^{\infty}\Gamma_{nij}q_i(t)q_j(t)+\sum_{i,j.k=1}^{\infty}\Lambda_{nijk}q_i(t)q_j(t)q_k(t)\\&+\sum_{i=1}^{\infty}g_l c_1\dot{q}_i(t-\tau)+\sum_{i,j=1}^{\infty}g_l c_2 q_i(t)\dot{q}_j(t-\tau)=f_n\cos(\Omega t),\end{aligned}\tag{4}$$

where,

$$\begin{aligned}\Gamma_{nij}&=-\alpha\int_0^1\left[\phi_j''(x)\int_0^1\phi_i^{'(x)}y'dx\right]\phi_n(x)dx-\frac{1}{2}\alpha\int_0^1\left[y''\int_0^1\phi_j^{'(x)}\phi_i^{'(x)dx}\right]\phi_n(x)dx,\\\Lambda_{nijk}&=-\frac{1}{2}\alpha\int_0^1\left[\phi_j''(x)\int_0^1\phi_k^{'(x)}\phi_i^{'(x)dx}\right]\phi_n(x)dx,\\f_n&=-\int_0^1 P(x)\phi_n(x)dx,\mu_n=\int_0^1 c\phi_n^2(x)dx,\\c_1&=-\alpha\phi_n(x_c)\int_0^1 y''\phi_n(x)dx,c_2=-\alpha\phi_n(x_c)\int_0^1\phi_i''(x)\phi_n(x)dx.\end{aligned}$$

In this study, the consideration is focused on the case of a single mode. For the sake of simplifying the description and facilitating the treatment of nonlinear terms for a more thorough analysis of the nonlinear response of the controlled suspended cable under superharmonic and subharmonic excitations, a new time scale $\imath=\omega_n t$ is introduced. Substituting it into Eq.(4), the following expression is obtained

$$\ddot{q}_n(t)+\omega_n^2 q_n(t)+2\mu_n\dot{q}_n(t)+\Gamma_{nnn}q_n^2(t)+\Lambda_{nnnn}q_n^3(t)+g_l c_1\dot{q}_n(t-\tau)+g_l c_2 q_n(t)\dot{q}_n(t-\tau)=f_n\cos(\Omega t).\tag{5}$$

3. Nonlinear Dynamic Response: 1/2 Subharmonic Resonance

In this section, the subharmonic resonance of the suspended cable is studied. Let

$$\Omega=2\omega_n+\varepsilon\sigma.\tag{6}$$

Let the solution to equation Eq.(5) be

$$q_n(t;\varepsilon)=q_{n0}(T_0,T_1)+\varepsilon q_{n1}(T_0,T_1)+\mathrm{O}(\varepsilon^2),\tag{7}$$

where $T_i=\varepsilon^i t,(i=0,1)$, the coefficients of the damping term, nonlinear term, external excitation term, and control term are adjusted, given by

$$\begin{aligned}\mu_n&=\mathrm{O}(\varepsilon),\Gamma_{nnn}=\mathrm{O}(\varepsilon),\Lambda_{nnnn}=\mathrm{O}(\varepsilon^2),\\f_n&=\mathrm{O}(\varepsilon),g_l=\mathrm{O}(\varepsilon^2),\Omega=2\omega_n+\varepsilon\sigma,\sigma=\mathrm{O}(1),\end{aligned}\tag{8}$$

where $\varepsilon(0<\varepsilon\leq 1)$ is a small parameter, and σ is a tuning parameter.

Substituting Eq.(7) into Eq.(5) and setting the coefficients of ε equal on both sides, we obtain

$\mathrm{O}(\varepsilon^0)$

$$D_0{}^2 q_{n0}+\omega_n{}^2 q_{n0}=f_n\cos(\Omega t),\tag{9}$$

$\mathrm{O}(\varepsilon^1)$

$$D_0{}^2 q_{n1}+\omega_n{}^2 q_{n1}=-2D_0D_1q_{n0}-2\mu_n D_0 q_{n0}-\Gamma_{nnn}q_{n0}^2,\tag{10}$$

$O(\varepsilon^2)$

$$\begin{aligned} D_0^2 q_{n2} + {\omega_n}^2 q_{n2} =& -2D_0 D_2 q_{n0} - D_1^2 q_{n0} - 2D_0 D_1 q_{n1} - 2\mu_n D_0 q_{n1} - 2\mu_n D_1 q_{n0} \\ & - 2\Gamma_{nnn} q_{n0} q_{n1} - \Lambda_{nnnn} q_{n0}^3 - g_l c_1 D_0 q_{n0}(t-\tau) - g_l c_2 q_{n0} D_0 q_{n0}(t-\tau). \end{aligned} \tag{11}$$

Solving Eq.(9) yields

$$q_{n0} = A_n(T_1, T_2)\exp(i\omega_0 T_0) + E_n \exp(i\Omega T_0) + cc, \tag{12}$$

where $i = \sqrt{-1}$, $E_n = \frac{1}{2} f(\omega_n^2 - \Omega^2)^{-1}$, and cc represent the conjugate complex numbers of the preceding terms.

Substituting equation Eq.(12) into equation Eq.(10), we obtain the secular term

$$2i\omega_n D_1 A_n + 2i\omega_n \mu_n A_n + 2\Gamma_{nnn} E_n \bar{A}_n \exp(i\sigma T_1) = 0. \tag{13}$$

By eliminating the secular term in the equation, the solution of Eq.(10) is obtained as

$$\begin{aligned} q_{n1} =& \frac{2i\Omega\mu_n E_n}{\Omega^2 - {\omega_n}^2}\exp(i\Omega \mathrm{T}_0) + \frac{\Gamma_{nnn} A_n^2}{3{\omega_n}^2}\exp(2i\omega_n T_0) - \frac{\Gamma_{nnn} E_n^2}{{\omega_n}^2 - 4\Omega^2}\exp(2i\Omega \mathrm{T}_0) \\ & + \frac{2\Gamma_{nnn} E_n A_n}{\Omega^2 + 2\Omega\omega_n}\exp[i(\Omega + \omega_n)T_0] - \frac{\Gamma_{nnn}}{{\omega_n}^2} A_n \bar{A}_n - \frac{\Gamma_{nnn}}{{\omega_n}^2} E_n^2 + cc. \end{aligned} \tag{14}$$

Let

$$A_n(T_1, T_2) = \frac{1}{2} a_n(T_1, T_2)\exp[i\beta_n(T_1, T_2)], \tag{15}$$

where a_n and β_n in the equation are real functions of T_1 and T_2, substituting Eq.(15) into Eq.(13) and separating the real and imaginary parts, we get

$$\begin{aligned} D_1 a_n &= -\mu_n a_n + \frac{\Gamma_{nnn} E_n a_n}{\omega_n}\sin\gamma_n, \\ a_n D_1 \gamma_n &= \sigma a_n - \frac{2\Gamma_{nnn} E_n a_n}{\omega_n}\cos\gamma_n, \end{aligned} \tag{16}$$

where $\gamma_n = \sigma T_1 - 2\beta_n$.

Substituting Eq.(12) and Eq.(14) into Eq.(11), rearranging the equation and eliminating the secular term, we have

$$\begin{aligned} & 2i\omega_n D_2 A_n + D_1^2 A_n + 2\mu_n D_1 A_n + 2c_3 A_n + 8c_4 A_n^2 \bar{A}_n + \frac{4i\Omega\mu_n \Gamma_{nnn}}{\Omega^2 - {\omega_n}^2} E_n \bar{A}_n \exp(i\sigma T_1) \\ & + i\Omega g_l c_2 E_n \bar{A}_n \exp(i\sigma T_1 - i\Omega\tau) + i\omega_n g_l c_1 A_n \exp(-i\omega_n \tau) - i\omega_n g_l c_2 E_n \bar{A}_n \exp(i\sigma T_1 + i\omega_n \tau) = 0, \end{aligned} \tag{17}$$

where

$$c_3 = \left(\frac{2\Gamma_{nnn}^2}{\Omega^2 + 2\Omega\omega_n} - \frac{2\Gamma_{nnn}^2}{{\omega_n}^2} + 3\Lambda_{nnnn}\right)E_n^2, c_4 = \frac{3\Lambda_{nnnn}}{8} - \frac{5\Gamma_{nnn}^2}{12{\omega_n}^2}.$$

Differentiating Eq.(13) with respect to T_1, we obtain

$$2i\omega_n D_1^2 A_n + 2i\omega_n \mu_n D_1 A_n + 2i\sigma\Gamma_{nnn} E_n \bar{A}_n \exp(i\sigma T_1) + 2\Gamma_{nnn} E_n D_1 \bar{A}_n \exp(i\sigma T_1) = 0. \tag{18}$$

From equations Eq.(13) and Eq.(18), we obtain

$$D_1 \bar{A}_n = -\mu_n \bar{A}_n - \frac{i\Gamma_{nnn} E_n A_n \exp(-i\sigma T_1)}{\omega_n}, \tag{19}$$

$$D_1^2 A_n + 2\mu_n D_1 A_n = -\frac{\sigma\Gamma_{nnn} E_n \bar{A}_n \exp(i\sigma T_1)}{\omega_n} + \left(\frac{\Gamma_{nnn}^2 E_n^2}{\omega_n^2} - \mu_n^2\right)A_n. \tag{20}$$

Substituting equations Eq.(19) and Eq.(20) into Eq.(17), we obtain

$$\begin{aligned}&2i\omega_n D_2 A_n + 2c_5 A_n + 8c_4 A_n^2 \bar{A}_n - \frac{\sigma\Gamma_{nnn} E_n \bar{A}_n \exp(i\sigma T_1)}{\omega_n}\\&+ 4i\Omega\mu_n c_6 E_n \bar{A}_n \exp(i\sigma T_1) + i\Omega g_l c_2 E_n \bar{A}_n \exp(i\sigma T_1 - i\Omega\tau)\\&+ i\omega_n g_l c_1 A_n \exp(-i\omega_n\tau) - i\omega_n g_l c_2 E_n \bar{A}_n \exp(i\sigma T_1 + i\omega_n\tau) = 0,\end{aligned} \tag{21}$$

where

$$2c_5 = 2c_3 + \frac{\Gamma_{nnn}^2}{{\omega_n}^2} E_n^2 - \mu_n^2, c_6 = \frac{\Gamma_{nnn}}{\Omega^2 - {\omega_n}^2}.$$

Substituting Eq.(15) into Eq.(21) and separating the real and imaginary parts, we obtain

$$\begin{aligned}D_2 a_n =&\frac{\sigma\Gamma_{nnn}\Lambda_n a_n}{2\omega_n}\sin\gamma_n - \frac{2c_6\Omega\mu_n E_n}{\omega_n} a_n\cos\gamma_n - \frac{1}{2} g_l c_2 \Omega E_n a_n \cos(\gamma_n - \Omega\tau)\\&+ \frac{1}{2} g_l c_2 \omega_n E_n a_n \cos(\gamma_n + \omega_n\tau) - \frac{1}{2} g_l c_1 \omega_n a_n \cos(\omega_n\tau),\end{aligned} \tag{22}$$

$$\begin{aligned}a_n D_2\gamma_n =&\frac{\sigma\Gamma_{nnn} E_n a_n}{\omega_n}\cos\gamma_n + \frac{4c_6\Omega\mu_n E_n}{\omega_n} a_n\sin\gamma_n + \frac{1}{2} g_l c_2 \Omega E_n a_n \sin(\gamma_n - \Omega\tau)\\&- \frac{1}{2} g_l c_2 \omega_n E_n a_n \sin(\gamma_n + \omega_n\tau) - \frac{1}{2} g_l c_1 \omega_n a_n \sin(\omega_n\tau) - (2c_5 + 2c_4 a_n^2) a_n,\end{aligned} \tag{23}$$

when the condition

$$\dot{a} = \varepsilon D_1 a + \varepsilon^2 D_2 a = 0, a\dot{\gamma} = \varepsilon a D_1\gamma + \varepsilon^2 a D_2\gamma_n = 0, \tag{24}$$

is satisfied, we have

$$\begin{aligned}&2i\omega_n\frac{dA_n}{dt} + 2i\varepsilon\omega_n\mu_n A_n + 2\varepsilon^2 c_5 A_n + 8\varepsilon^2 c_4 A_n^2 \bar{A}_n\\&+ 2\varepsilon c_7 f \bar{A}_n \exp(2i\varepsilon\sigma t) + \varepsilon^2 i\omega_n g_l c_1 A_n \exp(-i\omega_n\tau) = 0,\end{aligned} \tag{25}$$

the steady-state solution can be obtained, where

$$\begin{aligned}c_7 =&\frac{1}{2(\omega_0^2 - \Omega^2)}\left[\left(\left[\Gamma_{nnn}\left(1 - \frac{\varepsilon\sigma}{2\omega_n}\right) + \varepsilon\frac{1}{2} g_l c_2 \Omega\sin(\Omega\tau) + \varepsilon\frac{1}{2} g_l c_2 \omega_n \sin(\omega_n\tau)\right)\right.\right.^2\\&\left.\left.+ \left(\frac{2\varepsilon\Omega\mu_n\Gamma_{nnn}}{\Omega^2 - {\omega_n}^2} + \varepsilon\frac{1}{2} g_l c_2 \Omega\cos(\Omega\tau) - \varepsilon\frac{1}{2} g_l c_2 \omega_n \cos(\omega_n\tau)\right)^2\right]^{\frac{1}{2}}.\end{aligned} \tag{26}$$

Substituting Eq.(15) into Eq.(25) and separating the real and imaginary parts, we obtain

$$\begin{aligned}\omega_n {a'}_n =& -\varepsilon\omega_n\mu_n a_n - \varepsilon c_7 f a_n \sin\gamma_n - \varepsilon^2\frac{1}{2} g_l c_1 \omega_n a_n \cos(\omega_n\tau),\\\omega_n a_n {\gamma'}_n =&\omega_n\sigma a_n - 2\varepsilon^2(c_5 + c_4 a_n^2) a_n - 2\varepsilon c_7 f a_n \cos\gamma_n - \varepsilon^2 g_l c_1 \omega_n a_n \sin(\omega_n\tau),\end{aligned} \tag{27}$$

where

$$\gamma_n = \varepsilon\sigma t - 2\beta + \arctan\frac{\frac{2\varepsilon\Omega\mu_n\Gamma_{nnn}}{\Omega^2 - {\omega_n}^2} + \varepsilon\frac{1}{2} g_l c_2 \Omega\cos(\Omega\tau) - \varepsilon\frac{1}{2} g_l c_2 \omega_n \cos(\omega_n\tau)}{\Gamma_{nnn}(1 - \frac{\varepsilon\sigma}{2\omega_n}) + \varepsilon\frac{1}{2} g_l c_2 \Omega\sin(\Omega\tau) + \varepsilon\frac{1}{2} g_l c_2 \omega_n \sin(\omega_n\tau)}. \tag{28}$$

Table 1
Geometry and material properties parameters of the suspended cable[40].

Density ρ(kg/m^3)	Elastic modulus E(Pa)	Cross-sectional area A(m^2)	Span L(m)	Damping ratio μ_n	Aspect ratio d
7800	$2 * 10^{11}$	$7.069 * 10^{-2}$	200	0.005	0.015

When $a_n' = \gamma_n' = 0$, there exists a steady-state motion. In this case, Eq.(27) yields

$$\begin{aligned} &\omega_n \mu_n a_n + \varepsilon \frac{1}{2} g_l c_1 \omega_n a_n \cos(\omega_n \tau) = -c_7 f a_n \sin\gamma_n, \\ &\frac{1}{2}\sigma\omega_n a_n - \varepsilon(c_5 + c_4 a_n^2) a_n - \varepsilon \frac{1}{2} g_l c_1 \omega_n a_n \sin(\omega_n \tau) = c_7 f a_n \cos\gamma_n. \end{aligned} \tag{29}$$

Here, there exists a trivial solution($a_n = 0$). By eliminating γ_n from the system of Eq.(29), the amplitude-frequency response equation for nontrivial solutions can be obtained as

$$\varepsilon c_4 a_n^2 = \frac{1}{2}\sigma_e \omega_n - \varepsilon c_5 \pm (c_7^2 f^2 - \omega_n^2 {\mu_e}^2)^{1/2}, \tag{30}$$

where

$$\sigma_e = \sigma - \varepsilon g_l c_1 \sin(\omega_n \tau), \mu_e = \mu_n + \frac{1}{2}\varepsilon g_l c_1 \cos(\omega_n \tau).$$

From the amplitude-frequency response Eq.(30), the excitation amplitudes at two critical bifurcation points can be obtained as

$$f_1 = \frac{[(\frac{1}{2}\sigma_e \omega_n - c_5)^2 + \omega_n^2 \mu_e^2]^{1/2}}{|c_7|}, f_2 = \frac{\omega_n \mu_e}{|c_7|}, \tag{31}$$

where f_1 is the excitation amplitude at the subcritical bifurcation point, and f_2 is the excitation amplitude at the supercritical bifurcation point.

The analysis of the subharmonic resonance response of the controlled cable is conducted using the fundamental parameters outlined in Table.1.The amplitude-frequency response curves of the controlled suspended cable under different time delays are presented in Fig.2. Assuming a control gain of $g_l = 0.001$ and f=0.02, as the time delay τ decreases, the response curve shifts upwards and to the left, indicating a reduction in the subharmonic resonance region.

Furthermore, the amplitude-frequency response curves exhibit multiple values, falling into two distinct scenarios: either only one trivial solution $a_n = 0$ or there are three solutions, including one trivial solution and two nontrivial solutions (one stable and one unstable). However, unlike the primary resonance[38] and superharmonic resonance, the subharmonic resonance does not exhibit a jump phenomenon. Moreover, even though the external excitation frequency is twice the natural frequency of the controlled system, the system response is still significant.

Fig.3 shows the amplitude-frequency response curves of the controlled cable under 1/2-subharmonic resonance with different control gains. At a time delay value of $\tau = \pi/2$ and f=0.02, as the control gain increases, the resonance domain decreases and exhibits a shift.

Fig.4 depicts the correlation between the excitation amplitude and the response amplitude under different excitation amplitudes and time delays. When a certain value of σ (frequency) is fixed and the excitation amplitude increases to a certain value f_2 (for example, when $\tau = \pi/4$ and $\sigma = -0.2$, $f_2 \approx 0.015$), the system becomes unstable, and a subcritical bifurcation occurs at that point. Subcritical bifurcation cannot be eliminated and can only be controlled by adjusting the parameter to change the position of the bifurcation point (increasing or decreasing the value of f_2 at the critical bifurcation point) to ensure that the system does not undergo subcritical bifurcation within a certain amplitude range, thereby maintaining stability.

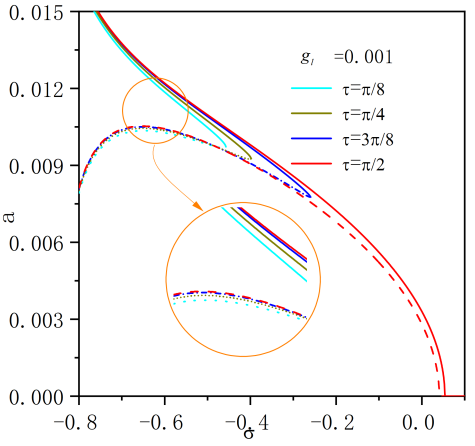

Figure 2: Amplitude-frequency response curves of 1/2 subharmonic resonance of the controlled suspended cable under different time delays.

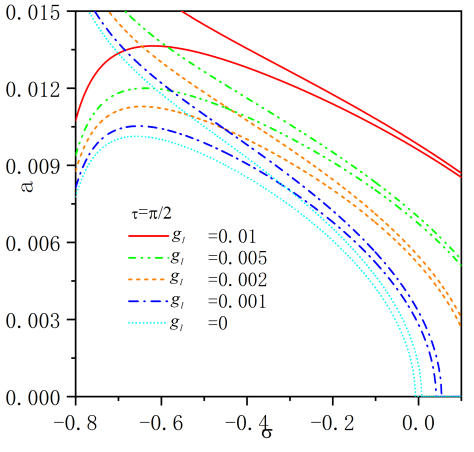

Figure 3: Amplitude-frequency response curves of 1/2 subharmonic resonance of the controlled suspended cable under different control gains.

When f=f_1 (for example, when $\tau = \pi/4$ and $\sigma = -0.2$), the system transitions from a stable trivial solution (trivial solution a=0) to three solutions (including one trivial and one unstable solution), resulting in a supercritical bifurcation. Meanwhile, it is evident that as the value of σ (frequency) increases and the time delay decreases, the response amplitude decreases significantly, and the position of the supercritical bifurcation also changes, and it can even be eliminated (as shown in the Fig.4 for $\tau = \pi/4$ and $\sigma = -0.2$).

Under the conditions of selecting a time delay of $\tau = \pi/2$ and a tuning parameter of $\sigma = -0.6$, Fig.5 illustrates the time-history curves and phase diagrams of 1/2 subharmonic resonance in a controlled suspended cable for control gains $g_l = 0.01$, $g_l = 0.005$ and $g_l = 0.001$, respectively. It is observed from the figures that the system response exhibits periodic motion. Notably, variations in control gain significantly affect the amplitude of the response. Specifically, as the control gain increases from $g_l = 0.001$ to $g_l = 0.01$, the peak amplitude of the response increases from 0.010 to 0.016, aligning with the trends presented in the amplitude-frequency curves in Fig.3. The increase in control gain leads to a higher response amplitude, indicating increased sensitivity of the system to external excitations. Concurrently, with the rise in control gain, the time required for the structure to reach a stable state decreases. This

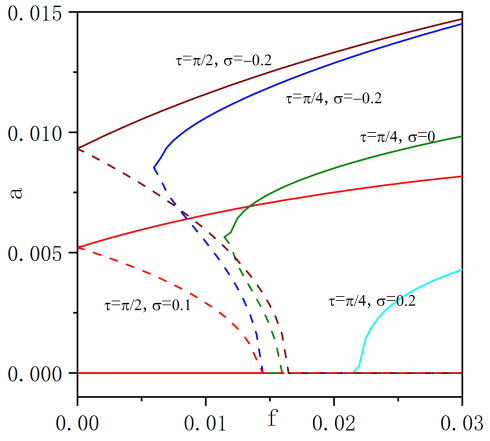

Figure 4: Relationship between the excitation amplitude and the response amplitude of 1/2 subharmonic resonance under different tuning parameters σ and time delays τ, where $g_l = 0.005$.

suggests that an appropriate gain value can achieve better control performance. Despite changes in control gain, the phase diagrams consistently depict periodic motion using a circular representation. It can be anticipated that, in most cases, adjusting the control gain does not alter the fundamental characteristics of the system or the periodic motion of nonlinear responses. Fig.6 provides a comparison of time history curves under three different control gains after narrowing the tuning parameter range and determining the time delay, once again emphasizing the significant impact of control gain on the system response. It is noteworthy that, with a decrease in control gain, the amplitude of the system response decreases, reaffirming the sensitivity of the system response amplitude to adjustments in control gain. Thus, by adjusting the control gain, the response amplitude of the suspended cable can be flexibly controlled, while maintaining the unchanged fundamental characteristics and periodic motion of nonlinear response. Through comparing the nonlinear response of the suspended cable under subharmonic excitation at zero degrees Celsius temperature difference with that in case.c of [34], it is observed that the time-delay feedback strategy effectively adjusts the system's amplitude and alters its stability, favoring vibration control of the structure.

In Fig.7, the corresponding frequency spectral analysis is presented for a control gain of $g_l = 0.001$. Through the analysis, it is observed that the system exhibits vibration peaks with two frequency components. The larger peak corresponds to the excitation frequency, while the smaller one represents the natural frequency, numerically demonstrating a 2:1 relationship. This underscores the subharmonic resonance characteristics present in the system.

In addition, in practical engineering applications, the tension force in the suspended cable assumes a pivotal role. Applications such as structural health monitoring, damage identification, cable force testing, and construction control all require the consideration of cable forces. Therefore, under the influence of both superharmonic or subharmonic excitations, the variations in cable forces in the suspended cable are defined as follows:

$$H_T = 1 + \alpha q \int_0^1 y'\varphi'(x)dx + \frac{\alpha}{2}q^2 \int_0^1 \varphi'(x)\varphi'(x)dx, \tag{32}$$

similar to the preceding context, here only the first-order symmetric mode is considered.

Fig.8 illustrates the dimensionless cable force time-history curves of the controlled suspended under subharmonic excitation with varying control gains. It can be observed that with an increase in control gain, the amplitude of the cable force correspondingly increases. This behavior is consistent with the scenarios described in the earlier Fig.3 frequency curve and Fig.5 time-history curve. Additionally, varying the control gains results in a distinct periodic variation trend in the cable force. Particularly, when the control gain $g_l = 0.01$, a significant influence on the cable force is observed, with the variation spanning from 5.8 to 14.7. As the control gain decreases, notably when $g_l = 0.001$, the impact on

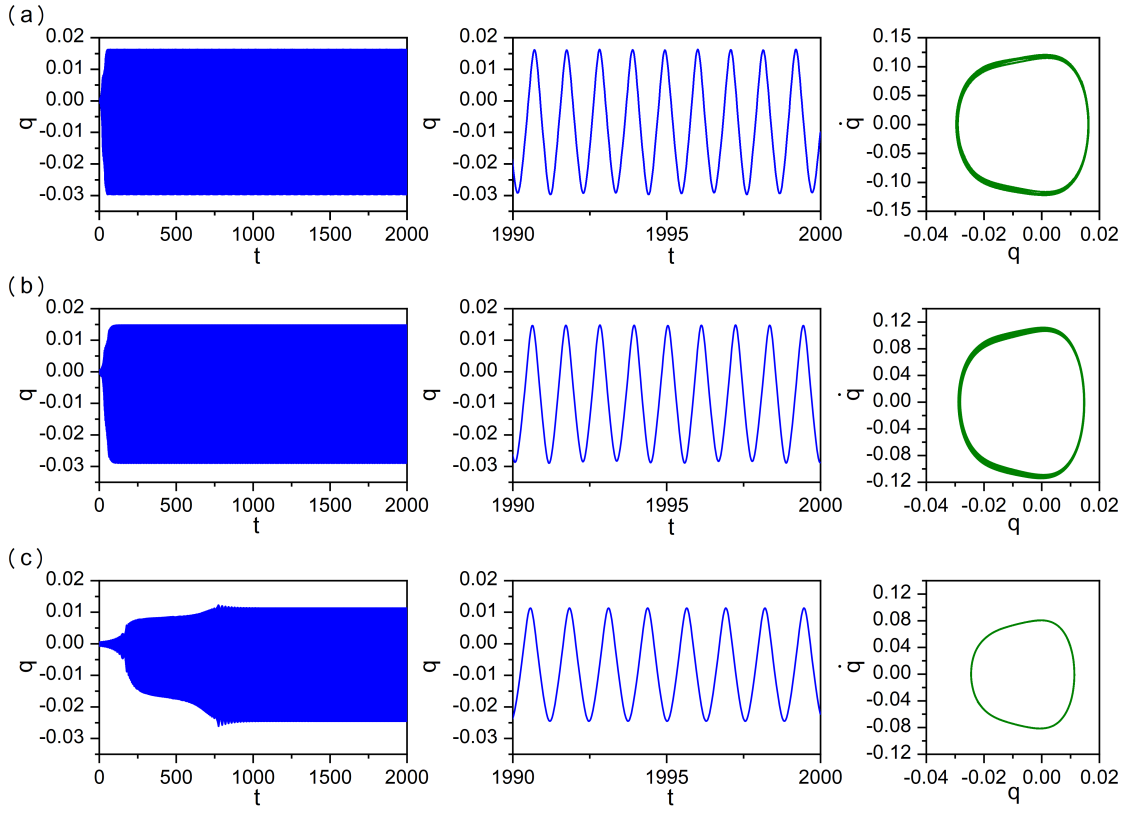

Figure 5: Time-history curve and phase diagram of 1/2 subharmonic resonance in a controlled suspended cable under different control gains at time delay $\tau = \pi/2$, (a)$g_l = 0.01$, (b)$g_l = 0.005$, (c)$g_l = 0.001$.

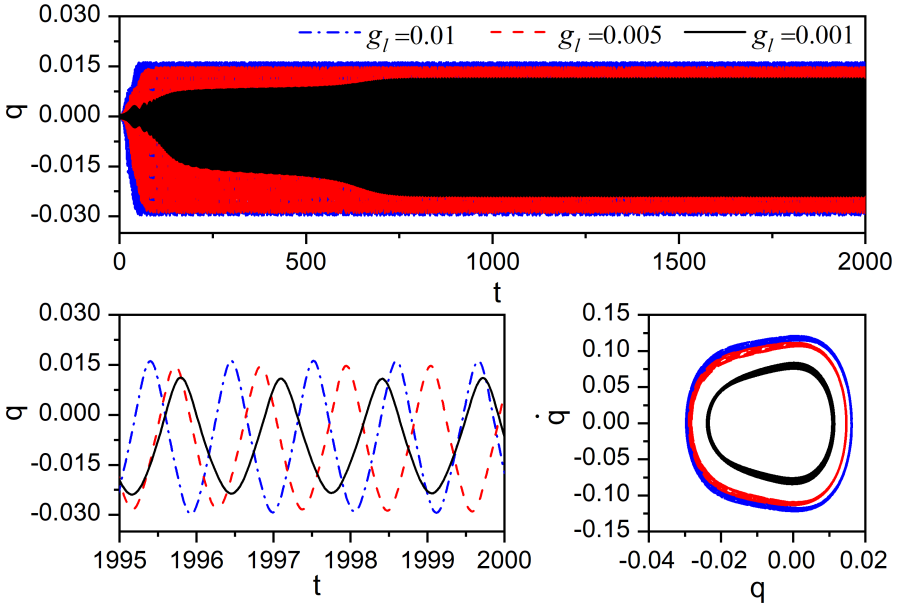

Figure 6: Time-history curve and phase diagram of 1/2 subharmonic resonance in a controlled suspended cable under different control gains at time delay $\tau = \pi/2$.

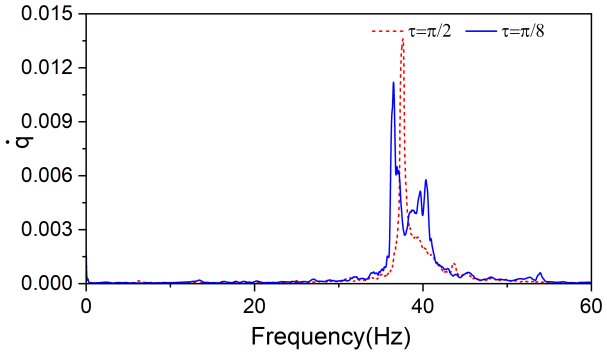

Figure 7: Spectral analysis of 1/2 subharmonic resonance in a controlled suspended cable with control gain $g_l = 0.001$.

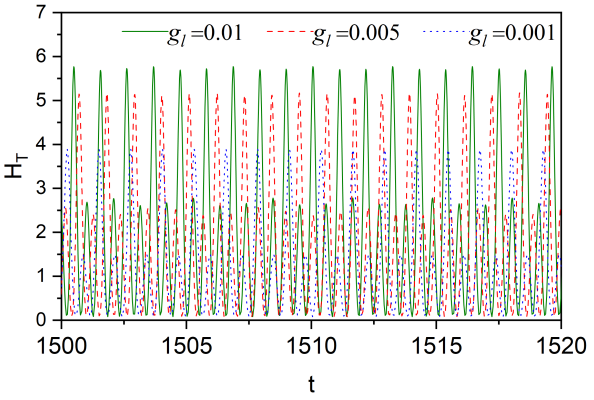

Figure 8: Time-history curves of cable forces under different control gains.

the cable force becomes smaller, with a variation range of [2.4,9.3]. Therefore, adjusting the size of the time-delay gain can be employed to reduce the amplitude of cable forces in the suspended cable.

Figure Fig.9 illustrates the impact of the control gain coefficient on the 1/2 subharmonic resonance of the system. It is evident from the figure that with the increase in the control gain g_l, the amplitude a correspondingly increases. However, the influence of different time delay values τ on the growth rate of amplitude a varies, particularly when g_l is relatively large, showcasing significant differences among the curves corresponding to different τ values.

The relationship between the time delay τ and the amplitude a of a suspended cable under 1/2 subharmonic excitation is illustrated in Fig.10. It is observed from the figure that a conspicuous periodic relationship exists between the amplitude a and the time delay τ, with significant and regular fluctuations within each cycle. This periodicity may be attributed to the phase difference introduced by the time delay, leading to variations in the system's periodic solutions. As a tuning parameter, the time delay modifies the interaction patterns of the internal vibration modes within a certain range of periods. Consequently, with the increase in time delay τ within this specified period range, the amplitude a first increases and then decreases, forming distinct peaks. The points of peak values are circled, representing instances where the system undergoes period doubling or chaotic phenomena, indicative of bifurcation, consistent with the linear depiction in Fig.4.Through these observations, the aforementioned content is validated. By adjusting the control gain g_l, resonance regions can be effectively avoided, significant structural vibrations can be suppressed, and a favorable control effect can be achieved.

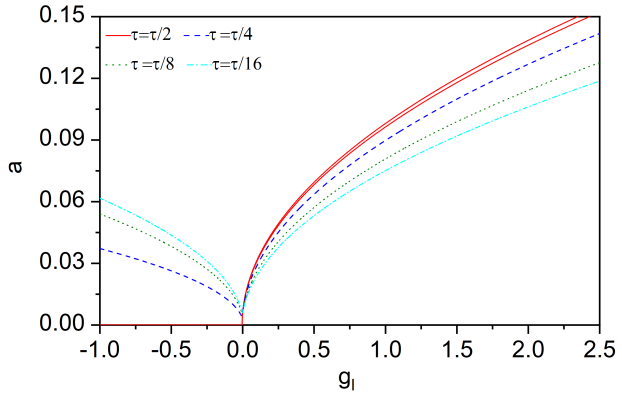

Figure 9: For $\sigma = -0.2$, the influence of control gain coefficient on the amplitude under 1/2 subharmonic excitation.

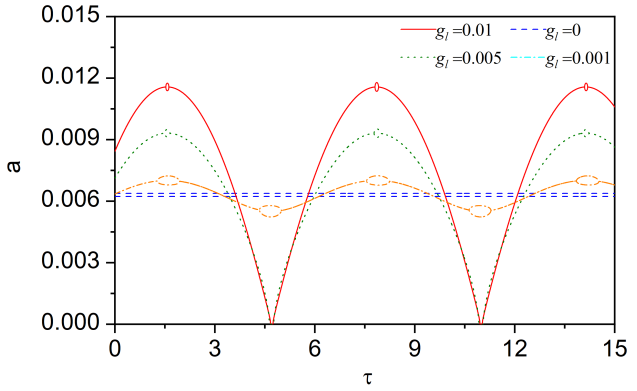

Figure 10: For σ=-0.2, the influence of time delay on the amplitude under 1/2 subharmonic excitation.

4. Nonlinear Dynamic Response: Second-Order Superharmonic Resonance

In this section, the superharmonic resonance of the suspended cable is studied. Let

$$\Omega = \frac{1}{2}\omega_n + \varepsilon\sigma. \tag{33}$$

From equations Eq.(10), Eq.(12), and Eq.(33), the secular term is obtained as

$$2i\omega_n D_1 A_n + 2i\omega_n \mu_n A_n - \Gamma_{nnn} E_n^2 \exp(2i\sigma T_1) = 0. \tag{34}$$

By eliminating the secular term in the equation, the secular term in the equation Eq.(10) is

$$\begin{aligned} q_{n1} =& \frac{2i\Omega\mu_n E_n}{\Omega^2 - {\omega_n}^2}\exp(i\Omega \mathrm{T}_0) + \frac{\Gamma_{nnn}A_n^2}{3{\omega_n}^2}\exp(2i\omega_n T_0) + \frac{2\Gamma_{nnn}E_n\bar{A}_n}{\Omega^2 - 2\Omega\omega_n}\exp[i(\Omega-\omega_n)\mathrm{T}_0] \\ &+ \frac{2\Gamma_{nnn}E_nA_n}{\Omega^2 + 2\Omega\omega_n}\exp[i(\Omega+\omega_n)T_0] - \frac{\Gamma_{nnn}}{{\omega_n}^2}A_n\bar{A}_n - \frac{\Gamma_{nnn}}{{\omega_n}^2}E_n^2 + cc. \end{aligned} \tag{35}$$

Substituting equations Eq.(12) and Eq.(35) into equation Eq.(11), rearranging the equation and eliminating the secular term, we have

$$\begin{aligned} &2i\omega_n D_2 A_n + D_1^2 A_n + 2\mu_n D_1 A_n + 2c_3 A_n + 8c_4 A_n^2 \bar{A}_n + \frac{4i\Omega\mu_n \Gamma_{nnn}}{\Omega^2 - {\omega_n}^2} E_n^2 \exp(2i\sigma T_1) \\ &+ i\omega_n g_l c_1 A_n \exp(-i\omega_n \tau) + i\Omega g_l c_2 E_n^2 \exp(2i\sigma T_1 - i\Omega\tau) = 0, \end{aligned} \tag{36}$$

where

$$c_3 = (\frac{2\Gamma_{nnn}^2}{\Omega^2 - 2\Omega\omega_n} + \frac{2\Gamma_{nnn}^2}{\Omega^2 + 2\Omega\omega_n} - \frac{2\Gamma_{nnn}^2}{{\omega_n}^2} + 3\Lambda_{nnnn})\mathrm{E}_n^2, c_4 = \frac{3\Lambda_{nnnn}}{8} - \frac{5\Gamma_{nnn}^2}{12{\omega_n}^2}.$$

Taking the derivative of Eq.(34) with respect to T_1, we obtain

$$2i\omega_n D_1^2 A_n + 2i\omega_n \mu_n D_1 A_n + 2i\sigma\Gamma_{nnn} E_n^2 \exp(2i\sigma T_1) = 0. \tag{37}$$

From equations Eq.(34) and Eq.(37), we have

$$D_1 A_n = -\mu_n A_n + \frac{i\Gamma_{nnn} E_n^2 \exp(2i\sigma T_1)}{2\omega_n}, \tag{38}$$

$$D_1^2 A_n + 2\mu_n D_1 A_n = \frac{i\Gamma_{nnn}\mu_n - 2\sigma\Gamma_{nnn}}{2\omega_n} E_n^2 \exp(2i\sigma T_1) - \mu_n^2 A_n. \tag{39}$$

Substituting Eq.(38) and Eq.(39) into Eq.(36), we get

$$\begin{aligned} &2i\omega_n D_2 A_n + 2c_5 A_n + 8c_4 A_n^2 \bar{A}_n - \frac{i\Gamma_{nnn}\mu_n - 2\sigma\Gamma_{nnn}}{2\omega_n} E_n^2 \exp(2i\sigma T_1) \\ &+ 4i\Omega\mu_n c_6 E_n^2 \exp(2i\sigma T_1) + i\omega_n g_l c_1 A_n \exp(-i\omega_n \tau) \\ &+ i\Omega g_l c_2 E_n^2 \exp(2i\sigma T_1 - i\Omega\tau) = 0, \end{aligned} \tag{40}$$

where

$$2c_5 = 2c_3 - \mu_n^2, c_6 = \frac{\Gamma_{nnn}}{\Omega^2 - {\omega_n}^2},$$

when the condition

$$\dot{a} = \varepsilon D_1 a + \varepsilon^2 D_2 a = 0, a\dot{\gamma} = \varepsilon a D_1 \gamma + \varepsilon^2 a D_2 \gamma_n = 0, \tag{41}$$

is satisfied, we have

$$\begin{aligned} &2i\omega_n \frac{dA_n}{dt} + 2i\varepsilon\omega_n \mu_n A_n + 2\varepsilon^2 c_5 A_n + 8\varepsilon^2 c_4 A_n^2 \bar{A}_n \\ &+ \varepsilon c_7 E_n^2 \exp(2i\varepsilon\sigma t) + \varepsilon^2 i\omega_n g_l c_1 A_n \exp(-i\omega_n \tau) = 0, \end{aligned} \tag{42}$$

which gives the steady-state solution.

Here,

$$c_7 = \left[\left(\left[\Gamma_{nnn} \left(1 - \frac{\varepsilon\sigma}{\omega_n} \right) + \varepsilon g_l c_2 \Omega \sin(\Omega\tau) \right)^2 + \left(\frac{\varepsilon\Gamma_{nnn}\mu_n}{2\omega_n} + \frac{4\varepsilon\Omega\mu_n\Gamma_{nnn}}{\Omega^2 - {\omega_n}^2} + \varepsilon g_l c_2 \Omega \cos(\Omega\tau) \right)^2 \right]^{\frac{1}{2}}. \tag{43}$$

Substituting Eq.(15) into Eq.(42) and separating the real and imaginary parts, we obtain

$$\begin{aligned} \omega_n {a'}_n &= -\varepsilon\omega_n\mu_n a_n - \varepsilon c_7 E_n^2 \sin\gamma_n - \varepsilon^2 \frac{1}{2} g_l c_1 \omega_n a_n \cos(\omega_n \tau), \\ \omega_n a_n {\gamma'}_n &= 2\sigma\omega_n a_n - \varepsilon^2 (c_5 + c_4 a_n^2) a_n - \varepsilon c_7 E_n^2 \cos\gamma_n - \varepsilon^2 \frac{1}{2} g_l c_1 \omega_n a_n \sin(\omega_n \tau), \end{aligned} \tag{44}$$

where

$$\gamma_n = 2\varepsilon\sigma t - \beta + \arctan\frac{\frac{\varepsilon\Gamma_{nnn}\mu_n}{2\omega_n} + \frac{4\varepsilon\Omega\mu_n\Gamma_{nnn}}{\Omega^2-{\omega_n}^2} + \varepsilon g_l c_2\Omega\cos(\Omega\tau)}{\Gamma_{nnn}(1-\frac{\varepsilon\sigma}{\omega_n}) + \varepsilon g_l c_2\Omega\sin(\Omega\tau)}. \tag{45}$$

When $a_n' = \gamma_n' = 0$, a steady-state motion exists. In this case, we can obtain the amplitude-frequency response equation from equation Eq.(44)

$$(2\sigma_e\omega_n a_n - \varepsilon(c_5 + c_4 a_n^2)a_n)^2 + (\omega_n\mu_e a_n)^2 = c_7^2 E_n^4, \tag{46}$$

where

$$\mu_e = \mu_n + \varepsilon\frac{1}{2}g_l c_1\cos(\omega_n\tau), \sigma_e = \sigma - \frac{1}{4}\varepsilon g_l c_1\sin(\omega_n\tau).$$

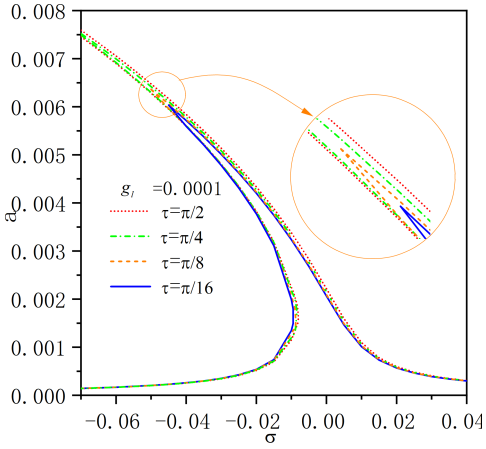

Figure 11: Amplitude-frequency response curves of second-order superharmonic resonance of the controlled suspended cable under different time delays.

Similarly, utilize the parameters from Table.1 to analyze the superharmonic resonance response of the controlled suspended cable. By deriving from Eq.(46), Fig.11 and Fig.12 reveal that the suspended cable exhibits soft spring characteristics (leftward deflection). As the time delay increases and the control gain decreases, the system response increases, displaying multi-valued and jump phenomena. Specifically, there are two possibilities for superharmonic resonance: either a stable nontrivial solution or three nontrivial solutions (including one unstable solution).

Under the conditions of selecting a control gain of $g_l = 0.0001$, f=0.02 and a tuning parameter of $\sigma = -0.02$, Fig.13 presents the time-history curves and phase diagrams of the controlled cable's second-order superharmonic resonance for $\tau = \pi/2$, $\tau = \pi/4$ and $\tau = \pi/8$, respectively. The figures reveal that the system continues to exhibit periodic motion. As the time delay decreases, the system response diminishes, effectively suppressing vibrations, consistent with the trends depicted in the amplitude-frequency response curve in Fig.11. In contrast to subharmonic resonance, the phase diagrams for superharmonic resonance consist of two circles, indicating the presence of jumping phenomena. Concurrently, as the time delay decreases, the time required for the structure to reach a stable state increases. By comparing the frequency response curves, time history plots, and phase diagrams of the suspended cable under supraharmonic excitation at a temperature difference of 0 degrees Celsius in case.a with those in [34], it is observed that employing time-delay control strategy enables adjustment of control gains and delay values, leading to a shift in the bifurcation points of the structure and ensuring stability within a certain range of amplitudes. Fig.14 shows the corresponding frequency spectrum analysis, also revealing two frequency values.

Fig.15 depicts the dimensionless cable force time-history curves of the controlled suspended cable under superharmonic excitation for various time delay values. It can be observed that as the time delay decreases, there

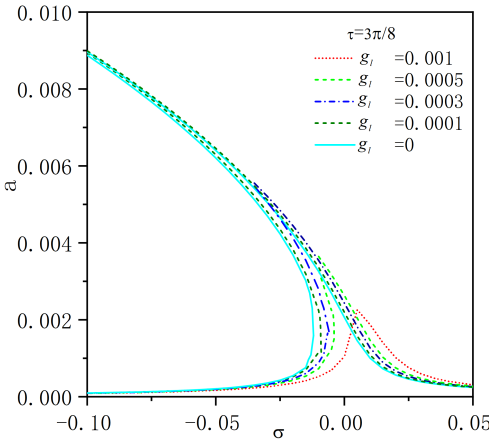

Figure 12: Amplitude-frequency response curves of second-order superharmonic resonance of the controlled suspended cable under different control gains.

is a corresponding reduction in the amplitude of force variation. This observation is consistent with the scenarios described in the earlier Fig.11 frequency curve and Fig.13 time-history curve. The cable force continues to exhibit a periodic variation trend even as the time delay values increase.

Fig.16 illustrates the impact of the control gain coefficient on the system's second-order superharmonic resonance. The figure clearly demonstrates that, starting from the origin, with the gradual increase in both positive and negative control gains, the system's amplitude correspondingly increases. This phenomenon indicates the nonlinear characteristics of the system. Similar to the subharmonic resonance scenario, different time delay values τ exert varying influences on the growth rate of amplitude a, especially when the control gain g_l is relatively large, leading to significant differences in the curves corresponding to different time delay values. Furthermore, the curves exhibit complex linearity at the origin, revealing the sensitivity of the system's dynamic response to the control gain parameter g_l within a specific range. This implies that the system may undergo a modal transition or stability mutation within this parameter range, marking the bifurcation point of the system solution.

Fig.17 illustrates the variation relationship between the time delay τ and the amplitude a of a suspended cable under second-order superharmonic excitation. Similar to Fig.10, the figure clearly displays the pronounced periodic dependence of the amplitude a on the time delay τ. Consequently, by investigating the relationship between the control gain g_l and the amplitude a, it is confirmed that the effective suppression of substantial vibrations in the suspended cable can be achieved through the appropriate adjustment of both time delay and control gain. This indicates that the method of time-delay control can prevent the system from entering unstable regions.

5. Conclusion

This paper investigates the controlled suspended cable's in-plane nonlinear dynamic model by employing a longitudinal time-delay feedback control strategy to study the superharmonic and subharmonic resonance responses of the cable. Based on the preceding discussions, the following conclusions can be drawn:

(1)Using time-delay feedback control can not only alter the amplitude but also change the system's stability, thereby effectively suppressing the vibration of the suspended cable.

(2)Adjusting control gain and time delay can shift the bifurcation points, ensuring system stability within a certain range of amplitudes. Therefore, optimal control of suspended cable structures under superharmonic and subharmonic excitations can be achieved by selecting appropriate control gains and time delays.

(3)Analysis of the control $g_l - a$ and $\tau - a$ diagrams reveals significant nonlinear behavior in the suspended cable under the influence of control gain and time delay. Moreover, it exhibits distinct periodicity and sensitivity under different conditions.

(4)The sensitivity of suspended cables to superharmonic and subharmonic excitations is significant.

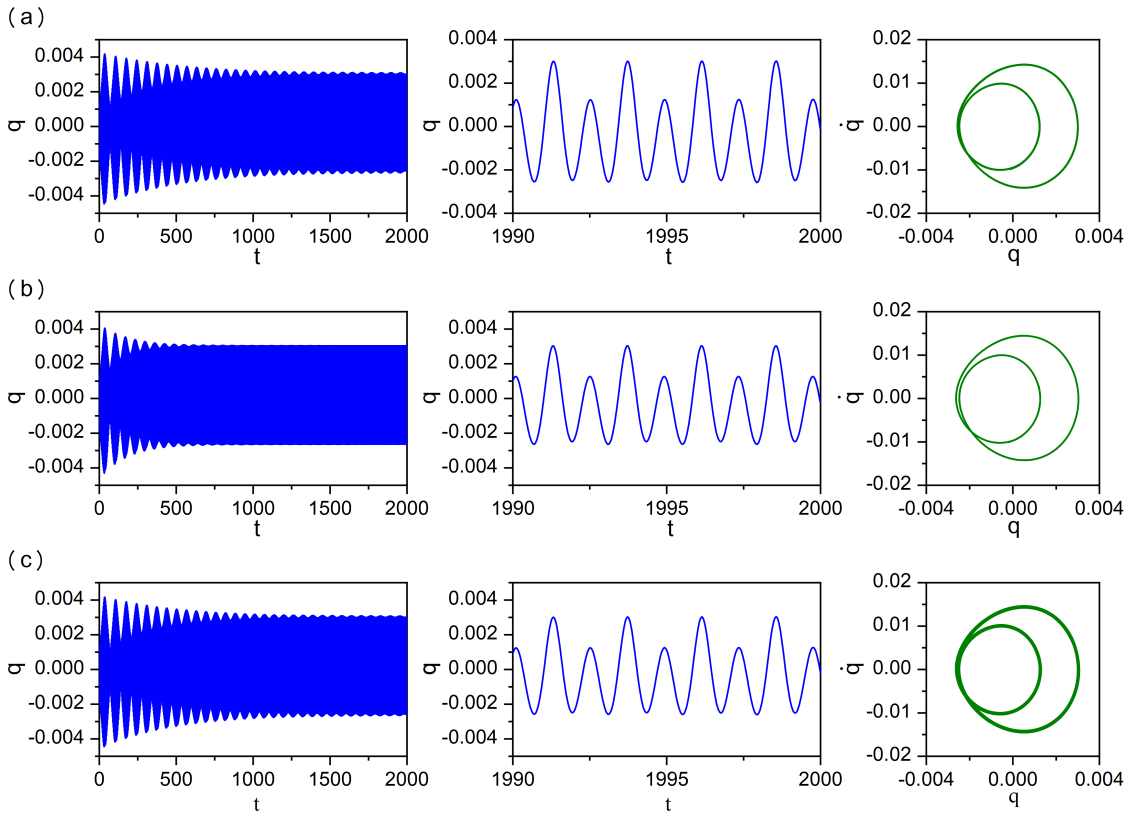

Figure 13: Time-history curve and phase diagram of second-order superharmonic resonance in a controlled suspended cable under different time delays at control gains $g_l = 0.0001$, (a)$\tau = \pi/2$, (b)$\tau = \pi/4$, (c)$\tau = \pi/8$.

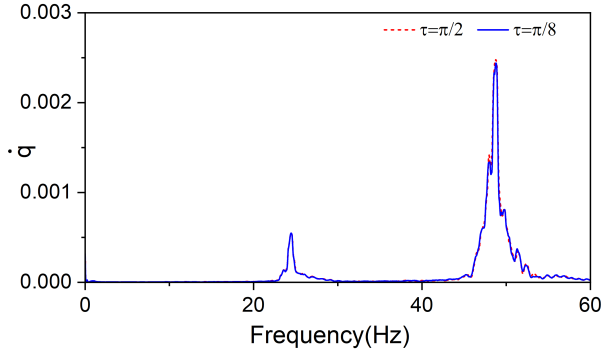

Figure 14: Spectral analysis of second-order superharmonic resonance in a controlled suspended cable with control gain $g_l = 0.0001$.

Therefore, time-delay vibration reduction technology proves to be an effective control strategy for managing the vibration of the suspended cable.

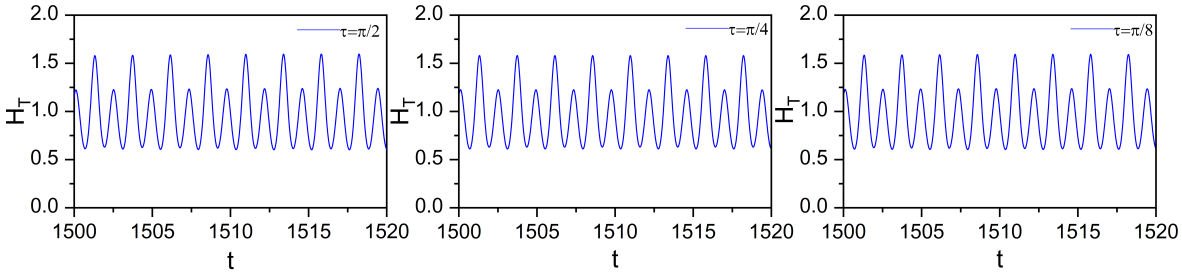

Figure 15: Time-history curves of cable forces under different time delay values.

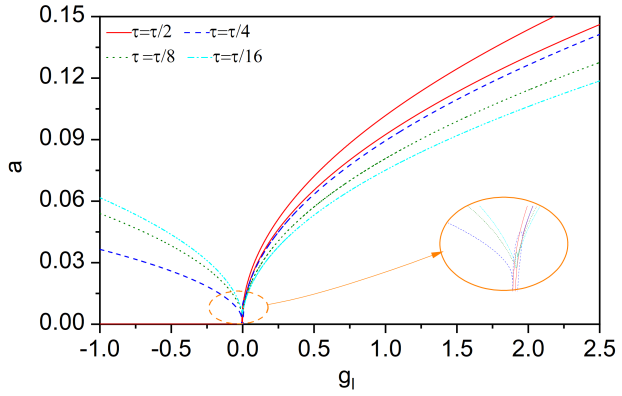

Figure 16: For σ=-0.2, the influence of control gain on the amplitude under second-order superharmonic excitation.

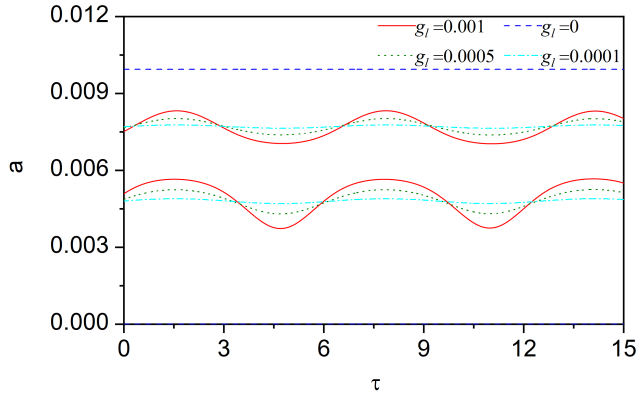

Figure 17: For σ=-0.2, the influence of time delay on the amplitude under second-order superharmonic excitation.

Acknowledgements

The study was supported by the Provincial Natural Science Foundation of Hunan (Grant No.2023JJ60527) and National Natural Science Foundation of China (Grant No.52078210) . The work of Prof. Lenci has been partially done within his belonging to the "Gruppo Nazionale per la Fisica Matematica".

References

[1] A. K. Agrawal, Y. Fujino, B. K. Bhartia, Instability due to time delay and its compensation in active control of structures, Earthquake engineering & structural dynamics 22 (3) (1993) 211–224.
[2] O. Flamand, Rain-wind induced vibration of cables, Journal of Wind Engineering and Industrial Aerodynamics 57 (2-3) (1995) 353–362.
[3] Y. Cong, Y. Jiang, H. Kang, W. Zhang, X. Su, Nonlinear dynamic analysis of vortex-induced resonance of a flexible cable, Nonlinear Dynamics (2023) 1–18.
[4] S. Li, Y. Deng, J. Huang, Z. Chen, Experimental investigation on aerodynamic interference of two kinds of suspension bridge hangers, Journal of Fluids and Structures 90 (2019) 57–70.
[5] Y. Deng, S. Li, Z. Chen, Unsteady theoretical analysis on the wake-induced vibration of suspension bridge hangers, Journal of Bridge Engineering 24 (2) (2019) 04018113.
[6] F. Di, L. Sun, L. Chen, Optimization of hybrid cable networks with dampers and cross-ties for vibration control via multi-objective genetic algorithm, Mechanical Systems and Signal Processing 166 (2022) 108454.
[7] H. Yamaguchi, H. D. Nagahawatta, Damping effects of cable cross ties in cable-stayed bridges, Journal of Wind Engineering and Industrial Aerodynamics 54 (1995) 35–43.
[8] W. Wang, X. Hua, X. Wang, J. Wu, H. Sun, G. Song, Mechanical behavior of magnetorheological dampers after long-term operation in a cable vibration control system, Structural Control and Health Monitoring 26 (1) (2019) e2280.
[9] H. Cao, A. Reinhorn, T. Soong, Design of an active mass damper for a tall tv tower in nanjing, china, Engineering Structures 20 (3) (1998) 134–143.
[10] Y. Jiang, W. Zhang, Y. Zhang, S. Lu, Nonlinear vibrations of four-degrees of freedom for piezoelectric functionally graded graphene-reinforced laminated composite cantilever rectangular plate with ppf control strategy, Thin-Walled Structures 188 (2023) 110830.
[11] T. Kobori, M. Takahashi, T. Nasu, N. Niwa, K. Ogasawara, Seismic response controlled structure with active variable stiffness system, Earthquake engineering & structural dynamics 22 (11) (1993) 925–941.
[12] C. T.-C. Nguyen, Mems technology for timing and frequency control, IEEE transactions on ultrasonics, ferroelectrics, and frequency control 54 (2) (2007) 251–270.
[13] S. Lu, Y. Jiang, W. Zhang, X. Song, Vibration suppression of cantilevered piezoelectric laminated composite rectangular plate subjected to aerodynamic force in hygrothermal environment, European Journal of Mechanics-A/Solids 83 (2020) 104002.
[14] V. Gattulli, M. Pasca, F. Vestroni, Nonlinear oscillations of a nonresonant cable under in-plane excitation with a longitudinal control, Nonlinear Dynamics 14 (1997) 139–156.
[15] V. Gattulli, R. Alaggio, F. Potenza, Analytical prediction and experimental validation for longitudinal control of cable oscillations, International Journal of Non-Linear Mechanics 43 (1) (2008) 36–52.
[16] H. Canbolat, D. Dawson, C. Rahn, S. Nagarkatti, Adaptive boundary control of out-of-plane cable vibration, Journal of Applied Mechanics, Transactions ASME 65 (1998) 963–969.
[17] Y. Zhang, S. K. Agrawal, P. Hagedorn, Longitudinal vibration modeling and control of a flexible transporter system with arbitrarily varying cable lengths, Journal of Vibration and Control 11 (3) (2005) 431–456.
[18] M. Pasca, F. Vestroni, V. Gattulli, Active longitudinal control of wind-induced oscillations of a suspended cable, Meccanica 33 (1998) 255–266.
[19] B. Wei, Z. Hu, X. He, L. Jiang, System-based probabilistic evaluation of longitudinal seismic control for a cable-stayed bridge with three super-tall towers, Engineering structures 229 (2021) 111586.
[20] H. Hu, Z. Wang, D. Schaechter, Dynamics of controlled mechanical systems with delayed feedback, Applied Mechanics Reviews 56 (3) (2003) 37–37.
[21] J. Peng, H. Xia, H. Sun, S. Lenci, Stability in parametric resonance of a controlled stay cable with time delay, International Journal of Structural Stability and Dynamics (2024) 2450233.
[22] N. Olgac, B. Holm-Hansen, A novel active vibration absorption technique: delayed resonator, Journal of sound and vibration 176 (1) (1994) 93–104.
[23] Y. Liu, N. Olgac, L. Cheng, Delayed resonator with multiple distributed delays–considering and optimizing the inherent loop delay, Journal of Sound and Vibration (2024) 118290.
[24] P. Zhu, M. Xiao, X. Huang, F. Zhang, Z. Wang, J. Cao, Spatiotemporal dynamics optimization of a delayed reactionâdiffusion musselâalgae model based on pd control strategy, Chaos, Solitons Fractals 173 (2023) 113751.
[25] Y. Yan, J.-X. Li, W.-Q. Wang, Time-delay feedback control of an axially moving nanoscale beam with time-dependent velocity, Chaos, Solitons Fractals 166 (2023) 112949.
[26] Q. Wu, M. Yao, M. Li, D. Cao, B. Bai, Nonlinear coupling vibrations of graphene composite laminated sheets impacted by particles, Applied Mathematical Modelling 93 (2021) 75–88.
[27] Q. Wu, M. Yao, Y. Niu, Nonplanar free and forced vibrations of an imperfect nanobeam employing nonlocal strain gradient theory, Communications in Nonlinear Science and Numerical Simulation 114 (2022) 106692.
[28] J. Warminski, D. Zulli, G. Rega, J. Latalski, Revisited modelling and multimodal nonlinear oscillations of a sagged cable under support motion, Meccanica 51 (2016) 2541–2575.

[29] G. Rega, Nonlinear vibrations of suspended cables part i: Modeling and analysis, Applied Mechanics Reviews 57 (6) (2005) 443–478.
[30] S. Mirhashemi, H. Haddadpour, Nonlinear dynamics of a nearly taut cable subjected to parametric aerodynamic excitation due to a typical pulsatile wind flow, International Journal of Engineering Science 188 (2023) 103865.
[31] C. Sun, X. Zhou, S. Zhou, Nonlinear responses of suspended cable under phase-differed multiple support excitations, Nonlinear Dynamics 104 (2) (2021) 1097–1116.
[32] W. Zhang, Y. Tang, Global dynamics of the cable under combined parametrical and external excitations, International Journal of Non-Linear Mechanics 37 (3) (2002) 505–526.
[33] K. Chen, K. Wang, X. Zheng, S. He, Modelling and analysis of the influence of in-plane vertical modes on the internal resonance of cable-stayed bridges, International Journal of Non-Linear Mechanics 145 (2022) 104114.
[34] Y. Zhao, C. Huang, L. Chen, Nonlinear planar secondary resonance analyses of suspended cables with thermal effects, Journal of Thermal Stresses 42 (12) (2019) 1515–1534.
[35] G. Zheng, J. Ko, Y. Ni, Super-harmonic and internal resonances of a suspended cable with nearly commensurable natural frequencies, Nonlinear Dynamics 30 (2002) 55–70.
[36] A. Nayfeh, J. Nayfeh, D. Mook, On methods for continuous systems with quadratic and cubic nonlinearities, Nonlinear Dynamics 3 (1992) 145–162.
[37] D.-L. Wu, C.-L. Tang, X.-P. Wu, Subharmonic and homoclinic solutions for second order hamiltonian systems with new superquadratic conditions, Chaos, Solitons Fractals 73 (2015) 183–190.
[38] Y. Tang, J. Peng, L. Li, H. Sun, X. Xie, Vibration control of nonlinear vibration of suspended cables based on quadratic delayed resonator, in: Journal of Physics: Conference Series, Vol. 1545, IOP Publishing, 2020, p. 012005.
[39] H. Irvine, Cable Structures, MIT Press series in structural mechanics, MIT Press, 1981.
[40] Y. Zhao, C. Huang, L. Chen, J. Peng, Nonlinear vibration behaviors of suspended cables under two-frequency excitation with temperature effects, Journal of Sound and Vibration 416 (2018) 279–294.